ISSN 0208-7774 TRIBOLOGIA 4/2018 p. 151–156

Sławomir WOŚ[*], Waldemar KOSZELA[*], Paweł PAWLUS[*]

THE EFFECT OF THE SHAPE OF OIL POCKETS ON THE FRICTION FORCE

WPŁYW KSZTAŁTU KIESZENI SMAROWYCH NA SIŁĘ TARCIA

Key words: textured surfaces, pin-on-disc, friction force, abrasive jet machining.

Abstract Tests were carried out using a pin-on-disc tester under starved lubrication conditions. To achieve a conformal contact, a special construction was used with an adjustable counter sample. Textured surfaces with two dimple patterns (spiral an radial) and four shapes (circle, oval, triangle, and chevron) were tested. The contact area was lubricated with L-AN-46 oil. Before the tests, surface topographies of the discs were measured by a white light interferometer Talysurf CCI Lite. Tests showed that, in starved lubrication conditions, oil pocket shape and pattern affected the friction force.

Słowa kluczowe: teksturowane powierzchnie, tester trzpień–tarcza, siła tarcia, obróbka strumieniowo-ścierna.

Streszczenie: Badania zostały przeprowadzone z wykorzystaniem testera typu trzpień–tarcza w warunkach ubogiego smarowania. Aby zapewnić warunki styku rozłożonego, została zastosowana specjalna konstrukcja z wahliwą przeciwpróbką. Badane powierzchnie tarczy teksturowano, aby uzyskać kieszenie smarowe o czterech kształtach ułożonych w dwóch szykach. Kieszenie smarowe miały kształty: okrągły, owalny, trójkątny i w kształcie zygzaka (jodełki). Strefę styku smarowano olejem L-AN-46. Przed próbami tribologicznymi wykonano pomiary struktury geometrycznej powierzchni tarcz z wykorzystaniem interferometru światła białego Talysurf CCI Lite. Przeprowadzone próby wykazały, że w warunkach ubogiego smarowania zarówno kształt kieszeni smarowych, jak ich szyk ma wpływ na opory tarcia.

INTRODUCTION

Surface texturing is one of the well-known methods of controlling friction **[L. 1]**. Various techniques can be applied for surface texturing. Laser texturing **[L. 2]** and burnishing **[L. 3]** are the most popular methods of dimples creation on sliding surfaces. Both numerical and experimental investigations are applied to select the best possible texture geometry. Simulation experiments based on the Reynolds equation show that the depth/diameter ratio should be between 0.12 to 0.14 **[L. 2]**. Small variations in the oil pocket shape affect the hydrodynamic lift **[L. 3]**. Results showed that a small variation in dimple dimensions were possible. Numerical investigations revealed that dimples of rectangular and triangular shape substantially affected the friction force **[L. 3]**. Results showed that, in some cases, oil pockets caused an increase in wear **[L. 3]**. Surface texturing can be combined with coating. A surface was coated with TiN and DLC layers **[L. 4]** prior to texturing, and, as a result, a prolonged lifetime and reduced friction were obtained. The friction coefficient was reduced by the additional coating from 0.1 to 0.05. Another complex approach was presented by Hsu et al. **[L. 5]**, which was that a textured surface was designed for both full and mixed lubrications. This texture had relatively large and shallow oil pockets creating hydrodynamic lift in full lubrication and smaller dimples of higher depth for mixed lubrication. Textured surfaces sometimes cannot give any positive effect. This case was observed when an oil was contaminated with small particles of Al_2O_3 and SiO_2**[L. 6]**. Additional particles caused high friction and wear of sliding elements. In most cases, researchers arbitrary selected circular oil pockets, both in numerical investigation and practical investigation. Most of such investigations are concentrated on pit-area ratio and depths of oil pockets **[L. 7, 8]**. Square oil pockets were numerically tested by Gropper et al. **[L. 9]**.

[*] Rzeszow University of Technology, 35-959 Rzeszow, Al. Powstancow Warszawy 12, Poland, e-mail: wosslawomir@prz.edu.pl.

These investigations were also focused on pit area ratios and oil pocket depths. It was found that, for most cases, optimum texturing parameters depend significantly on the operating conditions, and oil pockets parameters should be selected separately for a specific case. Due to the oil pockets presence, the oil film thickness increased by 12%. Shen and Khonsari **[L. 10]** searched for optimal oil pocket shape for both unidirectional and bidirectional sliding, with the use of the sequential quadratic programming (SQP). The resulting chevron type oil pockets were obtained for unidirectional sliding, while, for bidirectional sliding, each oil pocket consisted of pair of the trapezoid-like shapes. Similar investigations were carried out by Zhang et al. **[L. 11]** where, for unidirectional sliding, oil pockets in shapes of bullets and almonds were selected.

EXPERIMENTAL DETAILS

Tests were carried out using a pin-on-disc tester T-11. During tests, friction forces were measured as a function of time with the use of an extensometer sensor made by the Hottinger Company, of type S2, which a range up to 50 N and an accuracy class of 0.1. All tests were carried out at an ambient temperature of 21ºC and a normal force of 20 N. The revolving speed was adjusted for a contact track radius of 8 mm; therefore, the sliding speed for all tested samples was 0.4 m/s. The average pressure generated by the counter sample on the tested discs was 1.59 MPa. Revolving speed was controlled by an inductive position transducer, of the SCID-1 ZVN type. The test duration was determined by the number of revolutions of 10 000, and the sliding distance was 502.6 m. All tests were carried out in unidirectional sliding. Test conditions were selected to achieve mixed and boundary lubrication conditions. Such operating parameters are typically encountered for sliding guides with low loadings. The textured surfaces can be used for decreases in friction forces in sliding guides with the preservation of the sliding guide's biggest advantage, which is vibration dumping. Tested discs were made of 42CrMo4 steel, and they were heat treated to achieve a hardness of 50 HRC. The diameter of the disc was 25.4 mm. The disc surface before texturing was polished so that its roughness height determined by the Ra parameter was Ra 0.06 mm.

After polishing, the untextured areas were covered with a laser cutting masks with different dimple shapes and processed. The masks were made of engraving foil, strengthened with glass fibres, and cut with a 35W CO_2 laser. The laser beam area was circular with a 0.2 mm diameter, so all dimple shapes were limited by this value.

For abrasive jet machining, aluminium oxide was used as an abrasive. The grain size was between 100 µm and 120 µm. Compressed air was used as the energy transmitting medium. The working pressure was 0.6 MPa. Exposition time was 30 s. Oil pockets shown

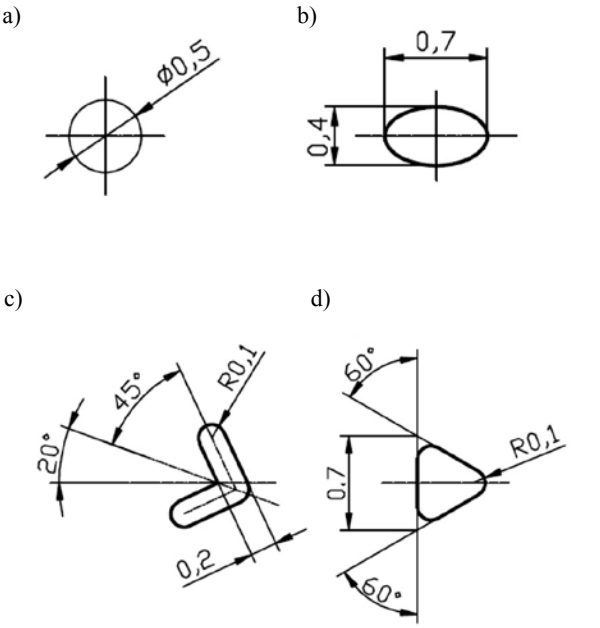

Fig. 1. Shapes of tested oil pockets: a) circle, b) oval, c) chevron, d) triangle

Rys. 1. Badane kształty kieszeni smarowych: a) koło, b) owal, c) zygzak, d) trójkąt

in **Fig. 1** were positioned in two patterns (spiral and radial), which have been used by the present authors in other works **[L. 8]**. By combining shapes and patterns, eight types of textures were produced. Masks shown in **Fig. 2** were used to obtain surface textures. All textures were made to obtain a pit ratio of 17% and to secure single oil pocket volumes at the same level for all used shapes. For comparison, the untextured disc was also tested. As a counter sample, a smaller disc was used. Its diameter was 5 mm with chamfering of 0.5 mm at 45º. The counter sample was also made from 42CrMo4 steel, and its hardness was 50 HRC. The counter sample was mounted on a pin so it could self-align with the co-acting surface (**Fig. 3**). The counter sample surface was also polished to the Ra parameter of 0.6 µm. Before tests, one drop (10.3 mm^3) of a lubricant was supplied to the centre of the friction zone. No further quantities of oil were added during test. The oil used during tests was L-AN-46 (kinematic viscosity at 40°C 46,0 mm^2/s, at 100°C 6,66 mm^2/s, viscosity index 96, ignition temperature min. 170°C, flow temperature max. -12°C, and density at 15^0C 880 kg/m^3). This volume of oil was sufficient to fill all oil pockets.

Spiral rows on textured disc (**Figs 2** and **4a**) were equally spaced, and the number of dimples on the disc circumference was 24, and the angle between rows was 15º. Radial rows of oil pockets (**Fig. 4b**) were obtained with an angle between rows of 12º and a radial spacing between dimple centres of 0,8 mm. **Figs 5** and **6** present contour plots and profiles of selected textured surfaces. Due to technical limitations in abrasive jet machining, oil pocket depth was in the range from 6 to 8 µm.

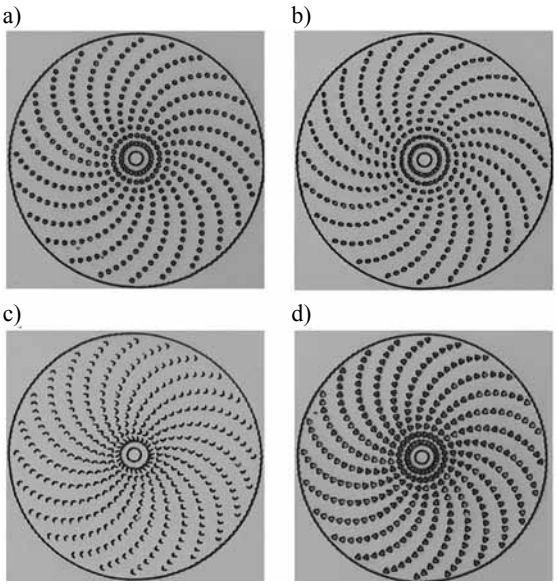

Fig. 2. Laser cut masks for spiral pattern and dimples of various shape: a) circle, b) oval, c) chevron, d) triangle

Rys. 2. Maskownice wycinane laserem dla szyku spiralnego i kształtu kieszeni smarowych: a) koła, b) owalnego, c) zygzaka, d) trójkątnego

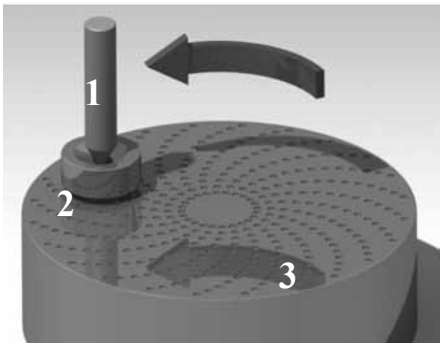

Fig. 3. A scheme of co-action of sliding pair: 1) holding pin, 2) counter sample, 3) textured disc

Rys. 3. Schemat współpracy pary ciernej 1) trzpień, 2) przeciwpróbka, 3) teksturowana próbka

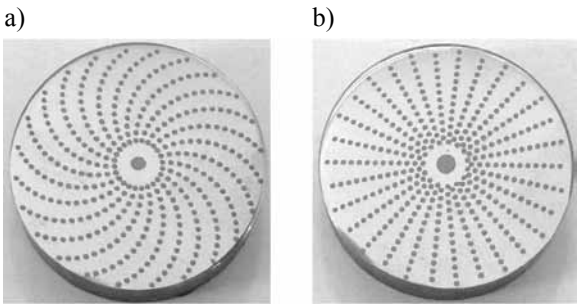

Fig. 4. Examples of textured discs: a) spiral pattern with circular oil pockets, b) radial pattern with circular oil pockets

Rys. 4. Przykładowe teksturowane tarcze: a) szyk spiralny z okrągłymi kieszeniami smarowymi, b) szyk promieniowy z okrągłymi kieszeniami smarowymi

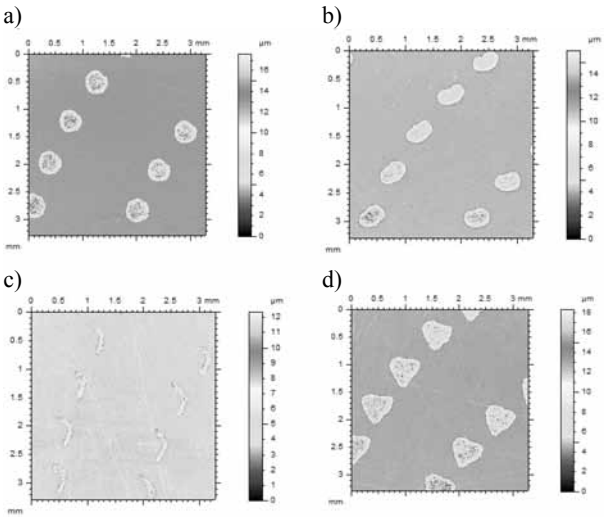

Fig. 5. Contour plots of different oil pockets shapes a) circle; b) oval, c) chevron, d) triangle

Rys. 5. Mapy konturowe przykładowych kieszeni smarowych: a) okrągłych, b) owalnych, c) w kształcie zygzaka, d) trójkątnych

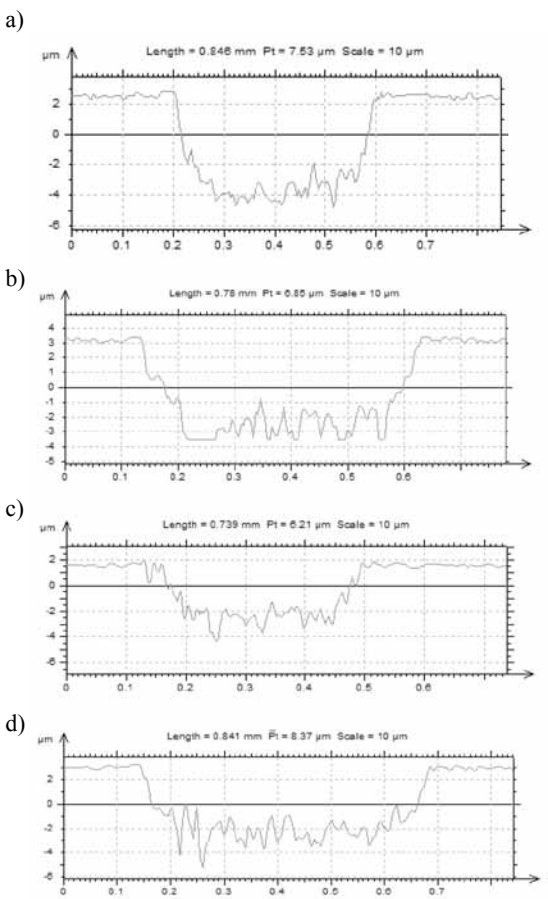

Fig. 6. Profiles of surfaces from textured discs with oil pockets, extracted along longer dimension: a) circular, b) oval, c) chevron, d) triangle

Rys. 6. Profile powierzchni teksturowanych dysków z widocznymi kieszeniami smarowymi wykonane wzdłuż większego wymiaru: a) okrągła, b) owalna, c) w kształcie zygzaka, d) trójkątna

RESULTS AND DISCUSSION

Figures 7 and **8** show the variation of the friction force with the number of revolutions for sliding pairs textured in spiral and radial patterns. All tests were repeated five times, except untextured discs (U), which was repeated eight times due to the friction force instability (**Fig. 9**). The untextured disc was a reference specimen. After comparison of the received friction force values, samples with radial rows array led to generally lesser stability compared to samples with a spiral array of oil pockets. Only the friction force of the assembly with a radial disc sample and chevron shape of oil pockets presented good stability without a tendency to adhesion (RC – radial;

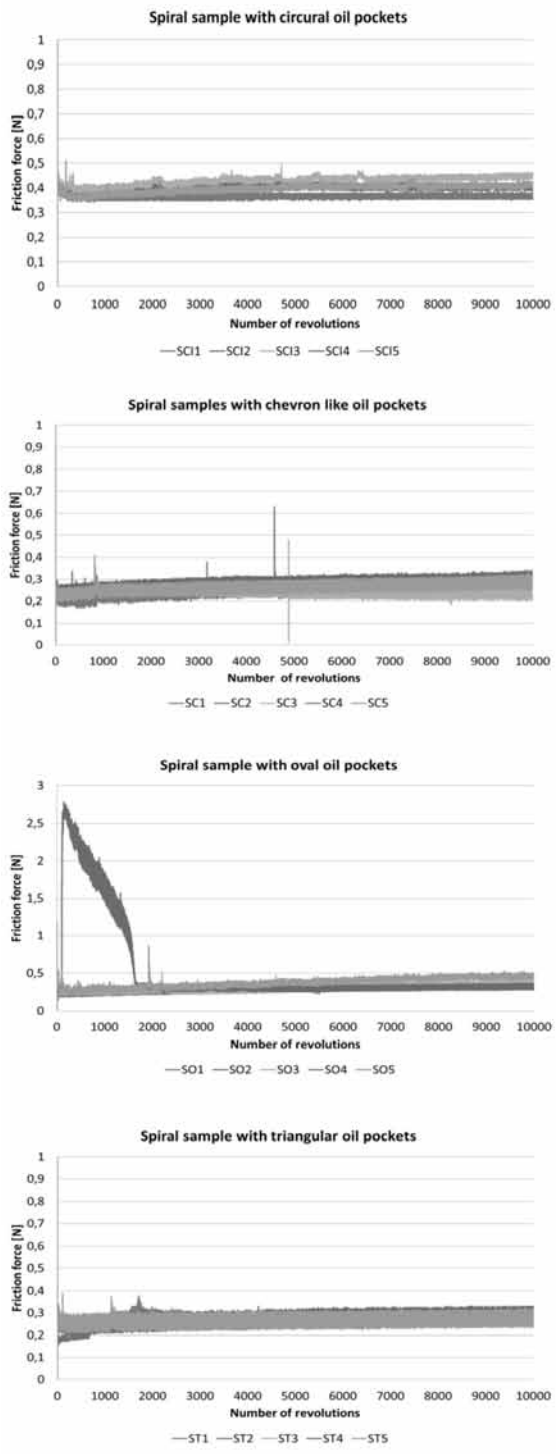

Fig. 7. Variation of the friction force with the number of revolution for sliding pairs with textured samples in spiral array

Rys. 7. Wykresy siły tarcia w funkcji liczby obrotów dla par ciernych teksturowanych w szyku spiralnym

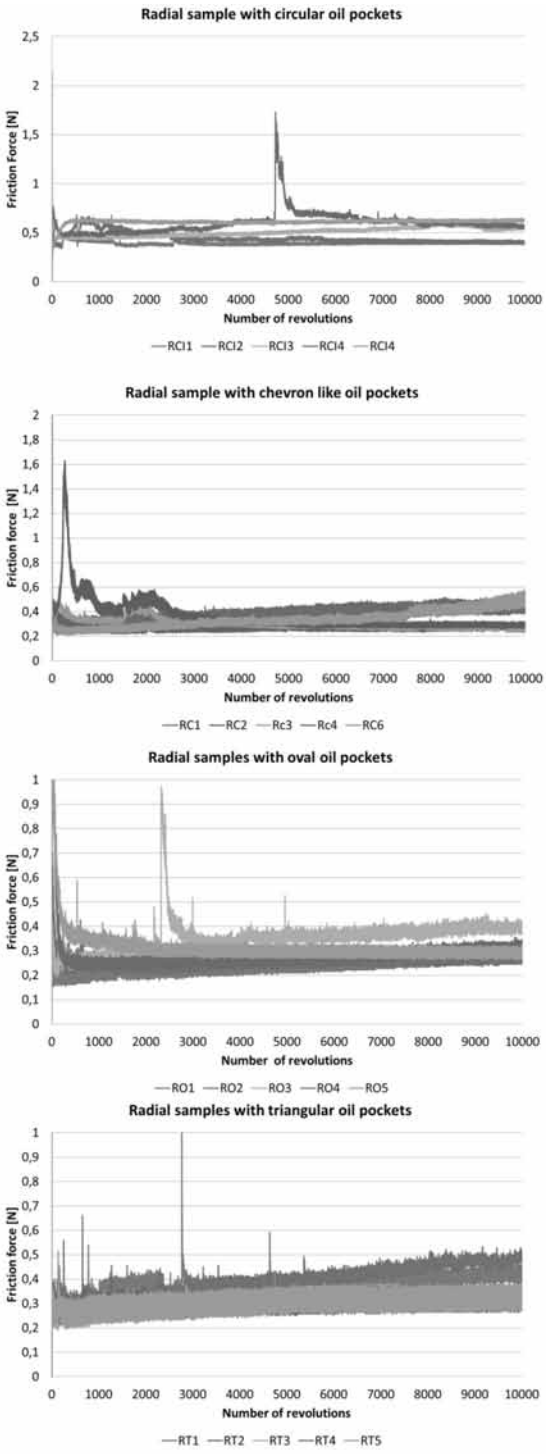

Fig. 8. Variation of the friction force with the number of revolution for sliding pairs with textured samples in radial array

Rys. 8. Wykresy siły tarcia w funkcji liczby obrotów dla par ciernych teksturowanych w szyku promieniowym

chevron) – **Fig. 8**. During tests, a tendency to a small increase in the friction force was observed. It was caused by inertial force that moved the lubricant to the outer radius of the disc. A slower friction force increase was registered for spiral array samples. The least stable results were obtained for untextured discs. This phenomenon was probably caused by the poor ability to maintain oil in the contact area. Textured surfaces have greater oil capacity, which helps to stabilize the friction force in starved lubrication conditions. Obtained friction forces were lower for all types of textured discs compared to untextured surfaces, and the average value of friction force was 0.79 N, the coefficient of friction (COF) was 0.0395. The smallest values of the friction force were obtained for the spiral pattern sample with triangular oil pockets. The average value of the friction force for this type of texture was 0.26 N (COF 0,013). The worst average value of the friction force was obtained for the radial sample with circular oil pockets (0.51 N; COF 0,0255). Variations in the tribological performance of assemblies of the same type of oil pocket shapes were the most evident for circular oil pockets where the average difference between friction forces was 0.11 N. This oil pocket shape was sensitive to oil pocket array changes.

Contrary chevron dimples presented the smallest sensitivity to oil pocket arrays (the average difference between friction forces for the two used arrays was about 0.06 N). Average values of the friction force shown in **Table 1** were calculated between 2000 and 10000 revolutions. The first part of friction was discarded during calculations, because of friction force instability during start-up.

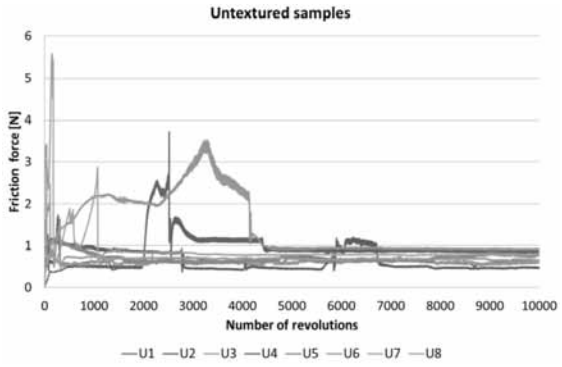

Fig. 9. Variation of the friction force with the number of revolution for sliding pairs with untextured samples

Rys. 9. Wykresy siły tarcia w funkcji liczby obrotów dla nieteksturowanych par ciernych

The received results are presented in **Figs 10, 11** and **12**. The coefficient of friction was calculated as the ratio between friction force and normal load. **Fig. 11** presents global average values of the friction coefficient. **Fig. 10** and **12** were added to highlight the differences between initial portion of the test and its final results. Received friction coefficients suggest that, in most cases, we obtained mixed lubrication conditions. However, for the assembly with untextured disc, we obtained mixed lubrication conditions with a constant decrease of the friction coefficient during the tests. Only in this case were scatters decreasing in time observed. This can be due to the wearing of micro-asperities. Due to the lack of oil pockets, the surface's ability to maintain the appropriate oil film thickness was low. This probably led to contact in region of micro-asperities and increased friction forces compared to sliding pairs with textured disc samples. In cases of textured surfaces, the values of the friction coefficient suggest that samples were working in mixed lubrication conditions with greater oil film thicknesses compared to the untextured disc. This ability and the creation of hydrodynamic lift by each oil pocket caused low friction coefficients. For all assemblies with textured discs, scatter and friction forces were increasing in time. This phenomenon can be explained by the constant decrease of oil volume due to inertial forces. These forces caused by rotary movement of the disc probably led to a slow but constant flow of oil into the outer radius of the disc. This could lead to a decrease of an oil film thickness and a decrease of the hydrodynamic lift.

The most stable result with the least scatter was achieved for the combination of triangular oil pockets and spiral array. However, the smallest stability was obtained for radial rows array with oil pockets of a circular shape. In most cases, the array of radial rows led to a greater friction force compared to the spiral array. The opposite results were obtained when oval oil pockets were used. Putting oil pockets in a radial array was beneficial only in this case.

Table 1. Friction force average values with scatter calculated as average value between 2000 and 10000 revolutions

Tabela 1. Wartości średnie siły tarcia wraz z rozrzutem obliczone jako średnie pomiędzy 2000 a 10000 obrotem

		Untextured disc
Friction force [N]	Max	1.362751
	Min	0.568307
	Average	0.797249

Oil pockets array			Oil pockets shape			
			Circular	**Oval**	**Chevron**	**Triangle**
spiral	Friction force [N]	Max	0.437202	0.393572	0.282946	0.277403
		Min	0.36552	0.286606	0.241642	0.248704
		Average	0.40274	0.319321	0.269998	0.262903
radial		Max	0.619938	0.374661	0.396114	0.417603
		Min	0.392283	0.244943	0.266037	0.3101
		Average	0.512895	0.291661	0.327857	0.348753

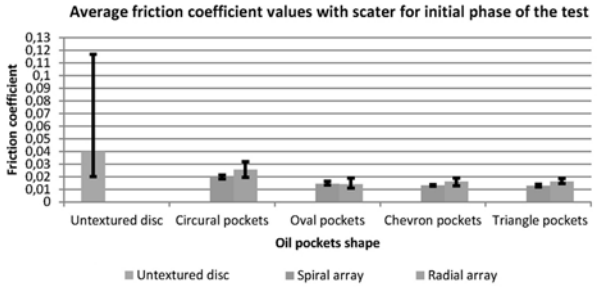

Fig. 10. Friction coefficient average values with scatters, calculated between 2000 and 4000 revolutions

Rys. 10. Średnie wartości współczynnika tarcia wraz z rozrzutem obliczone pomiędzy 2000 a 4000 obrotem

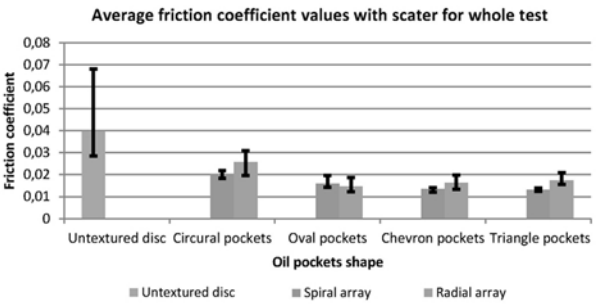

Fig. 11. Friction coefficient average values with scatters, calculated between 2000 and 10000 revolutions

Rys. 11. Średnie wartości współczynnika tarcia wraz z rozrzutem obliczone pomiędzy 2000 a 10000 obrotem

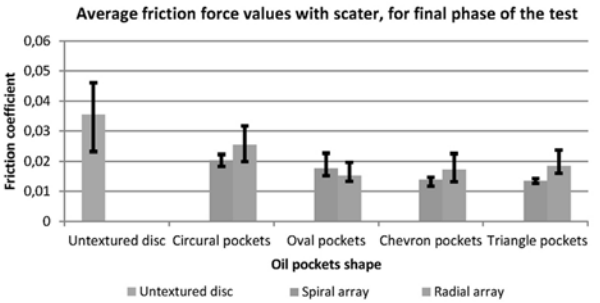

Fig. 12. Friction coefficient average values with scatters, calculated between 8000 and 10000 revolutions

Rys. 12. Średnie wartości współczynnika tarcia wraz z rozrzutem obliczone pomiędzy 8000 a 10000 obrotem

CONCLUSIONS

It was found during experimental investigations that the use of abrasive jet machining to create dimples on surfaces can improve the tribological performance of sliding elements in the presence of lubricant, even in starved lubrication conditions. In all tested cases, surface texturing resulted in a decrease in friction forces (in the best case of almost 67%). However, this effect was more visible for samples textured in the spiral pattern. Using different arrays of oil pockets was justified in a previous publication of the present authors **[L. 13]**. Chevron like oil pockets were the most universal shape after array of dimples. In both cases, the obtained friction forces were relatively small (only 3% worse than triangular oil pockets in the spiral array, and 11% worse than oval oil pockets in radial array).

REFERENCES

1. Anno J.N., Walowit J.A., Allen C.M.: Microasperity Lubrication, J. Lubr. Technol., vol. 90, no. 2, p. 351, 1968.
2. Ronen A., Etsion I., and Kligerman Y., Friction-Reducing Surface-Texturing in Reciprocating Automotive Components, Tribol. Trans., vol. 44, no. 3, pp. 359–366, Jan. 2001.
3. Burstein L., Ingman D.: Pore Ensemble Statistics in Application to Lubrication Under Reciprocating Motion, Tribol. Trans., vol. 43, no. 2, pp. 205–212, Jan. 2000.
4. Pettersson U., Jacobson S.: Influence of surface texture on boundary lubricated sliding contacts, Tribol. Int., vol. 36, no. 11, pp. 857–864, Nov. 2003.
5. Hsu S.M., Jing Y., Zhao F.: Self-adaptive surface texture design for friction reduction across the lubrication regimes, Surf. Topogr. Metrol. Prop., vol. 4, no. 1, p. 014004, Nov. 2015.
6. Koszela W., Dzierwa A., Galda L., Pawlus P.: Experimental investigation of oil pockets effect on abrasive wear resistance, Tribol. Int., May 2011.
7. Rom M., Müller S.: An effective Navier-Stokes model for the simulation of textured surface lubrication, Tribol. Int., vol. 124, pp. 247–258, Aug. 2018.
8. Takashima Y., Natsu W.: Study on Electrochemical Machining of Oil Pocket on Sliding Surface with Electrolyte Suction Tool, Procedia CIRP, vol. 42, pp. 112–116, 2016.
9. Gropper D., Harvey T.J., Wang L.: Numerical analysis and optimization of surface textures for a tilting pad thrust bearing, Tribol. Int., vol. 124, pp. 134–144, Aug. 2018.
10. Shen C., Khonsari M.M.: Numerical optimization of texture shape for parallel surfaces under unidirectional and bidirectional sliding, Tribol. Int., vol. 82, pp. 1–11, Feb. 2015.
11. Zhang H., Hua M., Dong G., Zhang D., Chen W., Dong G.: Optimization of texture shape based on Genetic Algorithm under unidirectional sliding, Tribol. Int., vol. 115, pp. 222–232, Nov. 2017.
12. Wos S., Koszela W., Pawlus P.: Tribological behaviours of textured surfaces under conformal and non-conformal starved lubricated contact conditions, Proc. Inst. Mech. Eng. Part J J. Eng. Tribol., vol. 229, no. 4, pp. 398–409, Apr. 2015.
13. Woś S., Koszela W., Pawlus P., The effect of oil pockets array on friction coefficient, Tribologia, vol. 4, pp. 97––105, 2017.